Published in final edited form as:
Acta Biomater. 2019 July 03; 96: 547–556. doi:10.1016/j.actbio.2019.07.001.

Concanavalin A-targeted mesoporous silica nanoparticles for infection treatment

Marina Martínez-Carmona[a,b], **Isabel Izquierdo-Barba**[a,b], **Montserrat Colilla**[a,b,*], **María Vallet-Regí**[a,b,*]

[a]Dpto. Química Inorgánica y Bioinorgánica Universidad Complutense de Madrid. Instituto de Investigación Sanitaria Hospital 12 de Octubre i+12. Plaza Ramón y Cajal s/n, 28040 Madrid, Spain

[b]CIBER de Bioingeniería, Biomateriales y Nanomedicina, CIBER-BBN, Madrid, Spain

Abstract

The ability of bacteria to form biofilms hinders any conventional treatment for chronic infections and has serious socio-economic implications. For this purpose, a nanocarrier capable of overcoming the barrier of the mucopolysaccharide matrix of the biofilm and releasing its loaded-antibiotic within this matrix would be desirable. Herein, we developed a new nanosystem based on levofloxacin (LEVO)-loaded mesoporous silica nanoparticles (MSNs) decorated with the lectin concanavalin A (ConA). The presence of ConA promotes the internalization of this nanosystem into the biofilm matrix, which increases the antimicrobial efficacy of the antibiotic hosted within the mesopores. This nanodevice is envisioned as a promising alternative to conventional treatments for infection by improving the antimicrobial efficacy and reducing side effects.

Keywords

Biofilm; Bacterial infection; Lectin; Mesoporous Silica Nanoparticles; Nanomedicine; Synergistic Combination; Targeting

1 Introduction

Presently, antimicrobial resistance (AMR) is a major threat to global health with serious socioeconomic implications [1,2]. Therefore, a post-antibiotic era is emerging to replace ineffective conventional antimicrobial treatments [3–5]. For this purpose, the combination of AMR and bacterial biofilm formation leads to infections that are almost unmanageable [6]. A biofilm is a bacterial community in which bacteria are embedded into an extracellular matrix mainly composed of polysaccharides. It renders the microorganisms a natural

*Corresponding authors: Fax: +34 394 1786; Tel.: +34 91 394 1843; vallet@ucm.es (M. Vallet-Regí) and mcolilla@ucm.es (M. Colilla).

Europe PMC Funders Author Manuscripts

Europe PMC Funders Author Manuscripts

mechanism of defense against external aggressions including antibiotics and the immune system [7].

MSNs have recently been used in nanomedicine owing to their efficiency in the host and their ability to protect and transport diverse drugs and locally release them on reaching the target tissue [8–10]. Further, MSNs have proven to be a multifunctional and versatile solution in the treatment of bacterial infections, as they have advantages at all stages of treatment, including early detection, drug release, targeting the bacteria or the biofilm, antifouling surfaces, and adjuvant capacity [11]. Specifically, once the biofilm has been formed, the use of these nanocarriers could be quite potent, as their surface can be functionalized with targeting agents, thereby increasing their affinity toward biofilms and favoring higher treatment efficacy [9–15].

Lectins such as ConA are glycoproteins present in a variety of organisms, and most of them are isolated from plant components [16]. Moreover, they have the ability to weakly bind to glycans with high specificity, hence forming glycoconjugates [17]. In reality, ConA has been successfully used to design antitumor drug-loaded nanoparticles that can selectively bind and internalize into cancer cells overexpressing membrane glycans [18,19]. Biocompatibility was also demonstrated, as no significant cell death was observed after incubation with MC3T3-E1 (mouse preosteoblastic) cells at concentrations up to 144 μg/mL [19]. As glycan-type polysaccharides are also present in the bacterial biofilm, we hypothesized that ConA could be used to target MSNs toward extracellular biofilm matrix. In fact, although the use of ConA for the treatment of infections due to planktonic bacteria is more widespread [20–22], its application once the biofilm is formed is very limited, and there appears to be a few publications on this subject. When uniquely present, ConA can be used for detection [23,24], as shown in a single publication in which ConA is part of a nanosystem used for treatment purposes [25]. In addition, this appears to be the initial demonstration of ConA anchorage to the surface of nanoparticles, which presents a significant antibiotic action, without the need for a loaded drug. However, it is true that the combined action of ConA and a therapeutic would be thought to intensify the antimicrobial character of the system. Herein, we report the design of a new nanoantibiotic consisting of MSNs loaded with an antimicrobial agent (LEVO) and grafted with ConA onto their outermost surface, which has been proved to selectively recognize and bind to certain glycans (Fig. 1).

2 Materials and Methods

2.1 Reagents

Tetraethylorthosilicate (TEOS, 98%), n-cetyltrimethylammonium bromide (CTAB, ≥99%), sodium hydroxide (NaOH, ≥98%), ammonium nitrate (NH_4NO_3, ≥98%), sodium carbonate (Na_2CO_3, ≥99.5%), hydrochloric acid (HCl, 37%), Rhodamine B isothiocyanate (RITC, ≥98%), (3-aminopropyl) triethoxysilane (APTES, ≥98%), N-(3-dimethylaminopropyl)-N′-ethylcarbodiimide hydrochloride (EDC, ≥98%), N-hydroxysulfosuccinimide sodium salt (sulfo-NHS, ≥98%), phosphate-buffered saline (PBS, 10x), phosphotungstic acid hydrate (PTA, reagent grade), and concanavalin A from *Canavalia ensiformis* (jack bean) (ConA, Type VI lyophilized powder) were purchased from Sigma-Aldrich (St. Louis, USA). 3-

(Triethoxysilyl)propylsuccinic anhydride (SATES, 95%) was purchased from ABCR (Karlsruhe, Germany). All other chemicals such as absolute ethanol were purchased from Panreac Química SLU (Castellar del Valles, Barcelona, Spain). All reagents were used as received without further purification. Ultrapure deionized water with a resistivity of 18.2 MΩ was obtained using a Millipore Milli-Q plus system (Millipore S.A.S., Molsheim, France). Levofloxacin (LEVO, $C_{18}H_{20}FN_3O_4$, 98 %w) was purchased from Sigma-Aldrich.

2.2 Characterization techniques

Powder X-ray diffraction (XRD) experiments were performed on a Philips X'Pert diffractometer equipped with Cu Kα radiation (wavelength 1.5406 Å) (Philips Electronics NV, Eindhoven, The Netherlands). XRD patterns were collected in the 2ϴ range between 0.6° and 8° with a step size of 0.02° and counting time of 5 s per step. Thermogravimetric (TG) measurements were performed using a PerkinElmer Pyris Diamond TG/DTA (California, USA), with 5 °C min^{-1} heating ramps, from room temperature (RT) to 600 °C. Fourier transform infrared spectroscopy (FTIR) was carried out using a Nicolet (Thermo Fisher Scientific, Waltham, MA, USA) Nexus spectrometer equipped with GoldenGate attenuated total reflectance (ATR) accessory (Thermo Electron Scientific Instruments LLC, Madison, WI, USA). Morphology, mesostructural order, and nanoparticle functionalization were studied by high-resolution transmission electron microscopy (HRTEM) with a JEOL JEM 1400 instrument, equipped with a CCD camera (JEOL Ltd., Tokyo, Japan). Sample preparation was performed by dispersing the sample in distilled water and subsequent deposition onto carbon-coated copper grids. A 1% PTA solution (pH 7.0) was used as the staining agent to visualize the organic coating around MSNs.

To determine the evolution of the size and surface charge of nanoparticles by dynamic light scattering (DLS) and zeta (ζ) potential measurements, respectively, a Zetasizer Nano ZS (Malvern Instruments, United Kingdom) equipped with a 633-nm "red" laser was used. DLS measurements were directly recorded in ethanolic colloidal suspensions. Measurements of ζ potential were recorded in aqueous colloidal suspensions. For this purpose, 1 mg of nanoparticles was added to 10 mL of solvent, followed by sonication for 5 min to obtain a homogeneous suspension. In both cases, measurements were recorded by placing 1 mL of the suspension (0.1 mg mL^{-1}) in DTS1070 disposable folded capillary cells (Malvern Instruments). The textural properties of the materials were determined by N_2 adsorption porosimetry by using a Micromeritics ASAP 2020 (Micromeritics Co., Norcross, USA). To perform N_2 measurements, 20-30 mg of each sample was previously degassed under vacuum for 24 h at 40 °C. Surface area (S_{BET}) was determined using the Brunauer-Emmett-Teller (BET) method, and pore volume (V_P) was estimated from the amount of N_2 adsorbed at a relative pressure of approximately 0.97. The pore size distribution between 0.5 and 40 nm was calculated from the adsorption branch of the isotherm by the Barrett-Joyner-Halenda (BJH) method. Mesopore size (D_P) was determined from the maximum of the pore size distribution curve.

2.3 Synthesis of pure-silica MSNs (MSN)

Bare MSNs, denoted as MSNs, were synthesized by the modified Stöber method using TEOS as the silica source in the presence of CTAB as the structure-directing agent. Briefly,

1 g of CTAB, 480 mL of H_2O, and 3.5 mL of NaOH (2 M) were added to a 1,000 mL round-bottom flask. The mixture was heated to 80 °C and magnetically stirred at 600 rpm. When the reaction mixture was stabilized at 80 °C, 5 mL of TEOS was added dropwise at a rate of 0.33 mL min^{-1}. The white suspension obtained was further stirred for 2 h at 80 °C. The nanoparticles were collected by centrifugation, washed twice with water and twice with ethanol, and stored in ethanol suspension. For cellular internalization studies, rhodamine-labeled MSNs were synthesized. For this purpose, 1 mg of FITC and 2.2 μL of APTES were dissolved in 100 μL of ethanol and allowed to react for 2 h. Then the reaction mixture was added to 5 mL of TEOS as previously described.

2.4 Functionalization of MSN with carboxylic acid groups (MSN_{SATES})

With the aim of preferentially grafting carboxylic acid groups to the external surface of MSNs, 500 mg of CTAB-containing MSNs was taken in a three-neck round-bottom flask and dried at 80 °C under vacuum for 24 h. Then 125 mL of dry toluene was added, and the flask was placed in an ultrasonic bath and subjected to several sonication cycles for 5 min until an adequate suspension of nanoparticles was achieved. Then 300 μL of SATES was added, keeping the reaction under nitrogen atmosphere at 90 °C for 24 h. The reaction mixture was centrifuged and washed three times with water and ethanol. The surfactant was removed by ionic exchange by soaking 1 g of nanoparticles in 500 mL of NH_4NO_3 solution (10 mg mL^{-1}) in ethanol (95%) at 65 °C overnight under magnetic stirring. The nanoparticles were collected by centrifugation, washed three times with ethanol, and stored in ethanol suspension.

2.5 ConA grafting to MSN_{SATES} (MSN_{ConA})

Sixteen milligrams of MSN_{SATES} was taken in a vial and suspended in 2 mL of PBS, pH 7.4, and subjected to several sonication cycles for 5 min until an adequate suspension was achieved. After that, 32 mg of EDC was added and the mixture was stirred at R.T. for 40 min. Then 14 mg of sulfo-NHS was added, and the reaction was stirred for 5 h; this was followed by addition of 32 mg of ConA, and the mixture was allowed to react overnight at R.T. Finally, the samples were centrifuged, washed twice with sterile 1x PBS, and suspended in fresh PBS.

2.6 Loading with levofloxacin (MSN@LEVO and MSN_{ConA}@LEVO)

MSN and MSN_{SATES} samples (12 mg) were obtained by centrifugation; these samples were suspended in 2 mL of LEVO solution (2.85 mg/mL) under stirring for 24 h. After that, MSN@LEVO and MSN_{SATES}@LEVO samples were centrifuged, washed once with EtOH and sterile 1x PBS, and suspended in 2 mL of fresh PBS.

Then 24 mg of EDC was added to (MSN_{SATES}@LEVO), and the mixture was stirred at R.T. for 40 min. Then 14 mg of NHS was added, and the reaction was further stirred for 5 h; this was followed by addition of 24 mg of ConA, and the reaction mixture was allowed to react overnight at R.T. Finally, the samples were centrifuged, washed twice with sterile 1x PBS, and suspended in 1 mL of fresh PBS, affording MSN@LEVO and MSN_{ConA}@LEVO. Both suspensions were divided as two batches: one was dried to perform release experiments and the other one was used for viability experiments. Quantitative determination of the loaded

Europe PMC Funders Author Manuscripts

LEVO was performed by elemental CHN chemical analyses in a PerkinElmer 2400 CHN and a LECO CHNS-932 thermo analyzer and TG analysis (TGA) in a PerkinElmer Pyris Diamond thermobalance. CHN analyses include low analytical ranges of 0.001–3.6 mg for carbon, 0.001–1.0 mg for hydrogen, 0.001–6.0 mg for nitrogen, and 0.001–2.0 mg for oxygen.

2.7 "*In vial*" cargo release assays

Dried MSN@LEVO and MSN_{ConA}@LEVO (4 mg) were suspended in 0.45 mL of 1x PBS and subjected to sonication until a good suspension was achieved. Then 170 μL of each nanoparticle suspension was filled into a reservoir cap sealed with a dialysis membrane (molecular weight cutoff: 12,000 g mol^{-1}), allowing the released LEVO molecules to pass into the cuvette (which was completely filled with 1x PBS), while the relatively large particles were held back. The experiment was performed in triplicate. The amount of LEVO released was determined by fluorescence measurements (λ_{exc} = 292 nm, λ_{em} = 494 nm) of the solution recorded on a BioTek Spectrofluorimeter (BioTek Instruments GmbH, Germany). Different calibration lines have been calculated for a concentration range of 12–0.01 μg/mL. To determine the effectiveness of the LEVO dosages released from the different MSNs against bacterial growth, 100 μL of each dosage was inoculated in 900 μL of PBS containing 10^8 bacteria per mL and incubated overnight. The presence or absence of bacteria, as well as their quantification, was determined by counting the colony-forming units (CFUs) in agar. For this purpose, 10 μL of this solution was seeded onto tryptic soy agar (TSA) and incubated at 37 °C overnight, followed by subsequent counting. Controls containing bacteria were also set, and the experiments were performed in triplicate.

2.8 Internalization assays in *E. coli* biofilm

In vitro targeting assays of LEVO-free nanosystems toward the bacterial biofilm were performed. For this purpose, *E. coli* biofilms were previously developed onto poly-D-lysine-coated round cover glasses by suspending the round cover glasses in a bacterial suspension of 10^8 bacteria per mL for 48 h at 37 °C under orbital stirring at 100 rpm. In this case, the medium used was 66% THB + 0.2% glucose to promote a robust biofilm formation. After that, the round cover glasses containing the biofilm were placed onto 24-well culture plates (CULTEK) containing 1.5 mL of new medium in each well. Then, 0.5 mL of a suspension of red-labeled MSN materials in PBS at final concentrations of 5, 10, and 50 μg/mL was added. After 90 min of incubation, the glass discs were washed three times with sterile PBS, and 3 μL/mL of Syto was added to stain the live bacteria, and 5 μL of calcofluor solution was added to stain the mucopolysaccharides of the biofilm (extracellular matrix) in blue to specifically determine the biofilm formation. Both reactants were incubated for 15 min at RT. Controls containing the bacterial biofilm were also set. Biofilm formation was examined using an Olympus FV1200 confocal microscope, and eight photographs (60X magnification) were taken for each sample.

2.9 Antimicrobial effects against gram-negative *E. coli* biofilm

Effectiveness of the LEVO-loaded nanosystems against the biofilm was also determined. For this purpose, two different assays were performed using mature *E. coli* biofilm. First, confocal assays were conducted, wherein *E. coli* biofilms were previously developed onto

poly-D-lysine-coated round cover glasses as done previously. Then, 0.5 mL of a suspension of different nanoparticles in THB at different concentrations (5, 10, and 50 μg/mL) was added. After 90 min of incubation, the glass discs were washed three times with sterile PBS, and 3 μL/mL of Live/Dead Bacterial Viability Kit (BacLight™) was added. In addition, 5 μL/mL of calcofluor solution was added to stain the extracellular matrix in blue to specifically determine the biofilm formation. Both reactants were incubated for 15 min at RT. Controls containing the bacterial biofilm were also set. Biofilm formation was examined using an Olympus FV1200 confocal microscope, and eight photographs (40X magnification) were taken for each sample. To perform quantitative analyses, the surface area covered with live bacteria (green) and extracellular matrix (blue) was calculated from eight images using ImageJ software (National Institutes of Health, Bethesda, MD). All images are representative of three independent experiments. Second, quantitative antibiofilm assays were carried out by calculating the reduction of CFU/mL. Previously, *E. coli* biofilms were seeded onto 24-well plates (CULTEK) by incubating 10^6 bacteria/mL for 48 h at 37 °C under orbital stirring at 100 rpm. In this case, the medium used was 66% THB + 0.2% glucose to promote a robust biofilm formation. After that, the biofilms were gently washed, and 1 mL of a suspension of MSN materials in THB at concentrations of 5, 10, and 20 μg/mL was added. After 24 h of incubation, the plates were washed three times with sterile PBS and sonication was applied for 1-10 min in a low-power bath sonicator (Selecta, Spain) to disperse the biofilm in a total volume of 1 mL of PBS. The sonicated sample was then serially diluted 7 times to 1:10 in a final volume of 1 ml. The experiments were performed in triplicate for each dilution of three different experiments. Quantification of the bacteria was carried out in a 1 mL volume using the drop plate method [26]. Five 10 μL drops of each dilution were inoculated on tryptic soy agar (TSA) (Sigma-Aldrich, USA) plates, which were incubated for 24 h at 37°C. The mean count of the 5 drops of each dilution was calculated, and then, the average counting for all dilutions was calculated.

2.10 Cell viability in presence of preosteoblastic cells

Cell culture studies were performed with the mouse osteoblastic cell line MC3T3-E1 (Subclone 4, CRL-2593; American Type Culture Collection, Manassas, VA, USA). First, cells were plated (24-well plates (CULTEK)) at a density of 20,000 cells·cm^{-2} in 1 mL of α-minimum essential medium containing 10% heat-inactivated fetal bovine serum and 1% penicillin (BioWhittaker Europe)−streptomycin (BioWhittaker Europe) at 37 °C in a humidified atmosphere of 5% CO_2 and incubated for 24 h. After that, different concentrations of MSNs, that is, 5, 10, and 50 μg/mL, were added to each culture. Cell viability after 24 h of incubation with different MSNs was analyzed. Cell growth was determined by the CellTiter 96 AQueous assay (Promega, Madison, WI, USA), a colorimetric method for determining the number of living cells in culture. The CellTiter 96 AQueous one-solution reagent [40 μL, containing 3-(4,5-dimethythizol-2-yl)-5-(3-carboxymethoxyphenyl)-2-(4-sulfophenyl)-2H-tetrazolium salt (MTS) and an electron-coupling reagent (phenazine ethosulfate) that allows its combination with MTS to form a stable solution] was added to each well, and the plates were incubated for 4 h. The absorbance at 490 nm was then measured on a Unicam UV-500 UV–visible spectrophotometer.

2.11 Statistical Analysis

All data are expressed as the mean ± standard deviation of a representative of three independent experiments carried out in triplicate. Statistical analysis was performed using Statistical Package for the Social Sciences (SPSS) version 19 software. Statistical comparisons were made by analysis of variance (ANOVA). The Scheffé test was used for post hoc evaluations of differences among groups. In all of the statistical analyses, $p < 0.05$ was considered as statistically significant.

3 Results and Discussion

3.1 Preparation and characterization of the nanosystems

The nanoantibiotic, denoted as MSN_{ConA}@LEVO, was synthesized through several steps (Fig. 2). Briefly, pure silica MSNs were synthetized by the well-known modified Stöber method [27] and externally functionalized by grafting an alkoxysilane-bearing carboxylic acid groups, which allows the final anchorage of ConA by reaction with the amine groups present in the protein. LEVO loading was carried out by the impregnation method in ethanol [13] and always before ConA grafting to prevent protein denaturation.

With the aim of confirming the chemical grafting of the different functional groups, MSN, MSN_{SATES}, and MSN_{ConA} were characterized by different techniques, and the results were compared after each reaction step. Using FTIR spectroscopy, we could follow the nanoparticle functionalization process. The change from a clean spectrum in the 1500-2000 cm^{-1} range of MSN to the presence of a signal at 1637 cm^{-1}, characteristic of the stretching vibration of acid groups, was observed in MSN_{SATES} (Fig. 3). Finally, in the FTIR spectrum of MSN_{ConA}, the amide bonds and NH out-of-plane bands were clearly seen, confirming the presence of this protein.

Measurements of ζ potential in aqueous colloidal suspensions showed representative changes on the superficial charge, with values of -21.5, -33.5, and -25.3 mV for MSN, MSN_{SATES}, and MSN_{ConA}, respectively.

The functionalization degree of the particles was calculated as the difference between TGA measures, finding 18% of SATES in MSN_{SATES} and 11% of protein in the final system MSN_{ConA}. As expected, the pore volume of the MSN suffers a decrease with increasing surface decoration. Thus, the specific surface area changes from 907 in the case of the naked material MSN to 240 m^2/g in the case of the complete system MSN_{ConA}.

Structural characterization by TEM (Fig. 4A-D) showed spherical nanoparticles with an average size of *ca.* 150 nm and a honeycomb mesoporous arrangement before and after functionalization and anchoring of the ConA. Moreover, all samples exhibited typical MCM-41 structure with a 2D hexagonal structure, which is also confirmed by XRD studies (Fig. S1). In this case, a small reduction in the intensity of the XRD peaks was observed for MSN_{SATES} and MSN_{ConA}, which is due to the slight order loss ascribed to the partial filling of the mesopore channels by the functionalization agent. In addition, after staining with 1% PTA, both samples that contained ConA (MSN_{ConA} and MSN_{ConA}@LEVO) showed that the protein covered all external surfaces of the nanoparticles, hence retaining the spherical

morphology even after loading win LEVO as shown in Fig. 4D. To acquire information of the mean size and stability of the nanosystems in solution, DLS measurements were recorded (Fig. S2). The measurements performed in Milli-Q H_2O showed a small increase in the hydrodynamic radius of the particles after functionalization with SATES and ConA.

3.2 *In vitro* LEVO release

The amount of LEVO loaded into nanoparticles was determined by elemental chemical analysis and TGA as 3.0 and 3.8% in weight for MSN@LEVO and MSN_{ConA}@LEVO, respectively, which is comparable with that mentioned in other studies based on silica mesoporous materials [12,28].

The *in vitro* drug release assays from different samples were carried out in PBS at 37°C under orbital stirring. Fig. 5 shows *in vitro* release profiles, which are expressed as accumulative drug release as function of time. The results indicate that both release curves can be adjusted to first-order kinetics, with the release rate faster and significantly higher after ConA grafting. Moreover, MSN@LEVO partially retains the loaded drug, with the maximum drug released, ca. 30%, after 48 h, which is in accordance with previous results [12,29]. On the contrary, MSN_{ConA}@LEVO released almost the total amount of loaded antibiotic after 5 days of assay. Previous studies have revealed that there is a strong interaction between the LEVO molecules and silica network in MSNs through hydrogen bonding between the zwitterionic form of this quinolone antibiotic at pH 7.4 and Si-OH groups of silica nanoparticles. Thus, the bare MSN sample partially retains the loaded LEVO, releasing approximately 30% after 2 days of assay. On the contrary, the presence of the ConA protein on the external surface promotes the interaction with LEVO molecules, which provokes drug departure from the mesopores, hence resulting in a faster antibiotic release.

Additionally, the biological activity of each antibiotic dose at different tested times was also evaluated by incubation with *E. coli* suspensions (10^8 bacteria/mL) and subsequent counting of colony-forming units (CFUs). Antimicrobial efficacy after 2 days and 5 days for MSN@LEVO and MSN_{ConA}@LEVO, respectively, was observed (Fig. S3), which was in good agreement with the results of kinetics studies.

In general, the drug release kinetics from mesoporous matrices are governed, primarily by drug diffusion processes throughout the matrix. Such drug diffusion processes are fitted, generally, to the Higuchi model. However, our results suggest that in addition to the drug diffusion process throughout the mesoporous matrix, a new component is governing the drug release kinetics. Specifically, this new component refers to the silica matrix–LEVO interactions, as it has been previously reported for other silica matrices.

3.3 *In vitro* internalization assays (targeting effect)

After demonstrating the antimicrobial capacity of the nanoantibiotic, the next step consisted in evaluating its bacterial biofilm-targeting efficacy. For this purpose, a preformed *E. coli* biofilm was incubated with different concentrations (5, 10, and 50 μg/mL) of nanoparticle suspensions. To solely evaluate the targeting effect, LEVO-free nanosystems were used, and confocal microscopy studies were conducted at different depths. To visualize the

nanoparticles, they were labeled in red with rhodamineB (RhB). Fig. 6 shows the internalization study of pristine MSN and MSN_{ConA} in a preformed *E. coli* biofilm after 90 min of incubation and 50 μg/mL of nanoparticles, chosen as a representative concentration. 3D confocal reconstruction showed a typical biofilm structure, live bacteria (green) covered by a protective polysaccharide matrix (blue), where MSNs are localized onto its surface (see white arrows). These results are consistent with those published in other studies. In 2014, Forier *et al.* investigated the effect of nanoparticle size in biofilm penetration, indicating that the cutoff size for optimal penetration was approximately 130 nm [30]. Specifically for MSN, D. L. Slomberg et al. synthesized nanoparticles of two sizes (14 and 150 nm) and studied their diffusion into *Pseudomonas aeruginosa* biofilm. They observed that diffusion was also size dependent, and although both MSNs penetrated into the biofilm, the process was higher and faster for the smaller ones [31]. Therefore, it was expected that our pristine MSN, whose size (150 nm) is within the limit described, would be mainly retained on the surface of the biofilm. On the contrary, it is surprising that MSN_{ConA} are able to penetrate the biofilm and be placed at different depth levels along the z-axis, suggesting that the effect of ConA is so powerful that it forces the internalization of nanoparticles whose size is theoretically inadequate. It is also worth mentioning that the MSN_{ConA} internalization degree is dose dependent, that is, the greater the concentration of the added nanoparticles, the higher is the amount of nanoparticles penetrating the biofilm (Fig. S4). MSN_{ConA}, with a ζ-potential of -25 mV, could have a strong electrostatic affinity toward the polysaccharide of the biofilm matrix [32]. Moreover, this targeting agent has shown a selective affinity to α-mannopyranosyl and α-glucopyranosyl residues present in the extracellular polysaccharide matrix, which could explain the internalization mechanism of the MSN_{ConA} system into bacterial biofilm [18].

3.4 Antimicrobial effects against gram-negative *E. coli* biofilm

Once the nanosystem has reached the biofilm, the anti-bacterial activity is determined by the physicochemical properties of the antimicrobial agent entrapped inside the nanosystem. Among others, LEVO, a synthetic fluoroquinolone antibacterial agent that inhibits the supercoiling activity of bacterial DNA gyrase, halting DNA replication, is a broad-spectrum antibiotic that provides clinical and bacteriological efficacy for a range of infections [33]. However, previous studies [12] have proved its inefficiency once the biofilm has been formed. To solve that, LEVO has been incorporated to the mesostructured arrangement of these targeted nanosystems to be released within the biofilm. For this purpose, a preformed *E. coli* biofilm was incubated with different concentrations (5, 10, and 50 μg/mL) of loaded nanoparticles (Fig. S5), with 10 μg/mL as the most optimum antibiofilm concentration.

Fig.7 shows the *in vitro* antimicrobial efficacy against preformed *E. coli* biofilms after 90 min of incubation with a suspension of 10 μg/mL of MSN, MSN@LEVO, MSN_{ConA}, and MSN_{ConA}@LEVO. The confocal microscopy image corresponding to control (Fig. 7C) shows a typical biofilm formed mainly by a mantle of live bacteria (green), with some dead bacteria (red) isolated and covered with a polysaccharide matrix represented in blue. The results show that samples treated with MSN present a small reduction in the biofilm (Fig. 7A). After treatment with MSN@LEVO (Fig. 7B), the reduction is more visible, with gaps appearing on its surface, probably due to a more superficial action of the antibiotic because

the particles practically did not penetrate into the biofilm but still showed a large amount of live bacteria. This reduction, in terms of percentage, corresponds to 50% of live bacteria and 70% for covered biofilm for bare MSN@LEVO, hence showing its antimicrobial inefficiency. On the contrary, this scenario totally changes after treatment with MSN_{ConA} (Fig. 7D), where a significant reduction of the biofilm is observed, even in the absence of the LEVO. Undoubtedly, this increase in antimicrobial capacity must be due to the presence of ConA. A study of the effect produced in the biofilm by the MSN_{ConA} sample shows a notable reduction in biofilm of 65% (green scatter) and 75% (blue scatter) (see Fig.7F). More experiments are necessary to elucidate the mechanism of ConA toxicity in the biofilm. However, we hypothesized that it could be similar to that observed for some other lectins [34–36]. Finally, Figure 7E shows that the biofilm treated with MSN_{ConA}@LEVO suffered a complete eradication, showing only a few scatter of bacteria (mostly dead/red). An in-depth analysis of the surface, calculated using ImageJ software, showed a reduction of almost 99.9% of live bacteria and almost 100% of blue-covered biofilm for the targeted nanosystems. These results evidence that the incorporation of ConA as a biofilm-targeting agent onto the MSN surface platform triggers complete biofilm destruction in combination with the antibiotic. In this sense, because of the penetration of these nanosystems into the biofilm and the release of the antibiotic inside it, a high antimicrobial efficacy is produced. On the contrary, treatment with bare MSN@LEVO provokes a reduction in the biofilm area, but the effect was significantly less effective owing to the lack of penetration into the biofilm. In addition, to determine the antibiofilm effect of MSN samples and confirm the effective dosage, the bacteria present in the biofilm after treatment were counted by the drop plate method. Fig. 8 shows the reduction in percentage of biofilm in terms of CFU per mL with regard to control after treatment. The obtained results show a notable reduction of 97.8% and 100% for 10 and 20 mg/mL for MSN_{ConA}@LEVO, respectively, which are in agreement with the results of confocal microscopy (Fig.7D). Note that the dose at 10 μg/mL shows a bacterial concentration of less than 10^2 bacteria/mL, which could be considered as an effective treatment [37].

3.5 Biocompatibility assays

The use of these nanocarriers for clinical applications in infection treatment requires that the designed material present excellent biocompatibility and absence of cytotoxicity. MSN is a biocompatible material that exhibits low toxicity and lack of immunogenicity and is degraded into nontoxic compounds (mainly silicic acid) in relatively short time periods [38]. Despite its lack of toxicity, the surface modification of this MSN could provoke toxicity because of enhanced uptake within the cells. To evaluate toxicity, MC3T3-E1 cells were incubated with different amounts of the MSNs in cell culture medium for 24 h. After incubation, cell viability was determined using the standard cell viability test by MTS reduction. The results showed that none of these empty materials exhibited cytotoxicity in either cell line (Fig. 9), which was in agreement with previous results [19].

4 Conclusions

In this work, a new class of targeting antimicrobial device based on mesoporous silica nanoparticles (MSNs) decorated with ConA and loaded with LEVO as the antibiotic has

Europe PMC Funders Author Manuscripts

been developed. The covalent grafting of ConA to MSNs (MSN_{ConA}) allows an effective penetration in gram-negative bacteria biofilm, which increases the antimicrobial efficacy of LEVO hosted in the mesopores. These findings demonstrate that the synergistic combination of biofilm internalization and antimicrobial agents into a unique nanosystem provokes a remarkable antimicrobial effect against bacterial biofilm. This nanocarrier is a promising alternative to the current available treatments for the management of infection. The next step in future studies is to determine its clinical relevance by *in vivo* models in wounds or after implant and prosthesis application.

Supplementary Material

Refer to Web version on PubMed Central for supplementary material.

Acknowledgments

This work was supported by European Research Council, ERC-2015-AdG (VERDI), Proposal No. 694160.

References

[1]. Taubes G. The Bacteria Fight Back. Science. 2008; 321:356–361. [PubMed: 18635788]

[2]. de Kraker MEA, Stewardson AJ, Harbarth S. Will 10 Million People Die a Year due to Antimicrobial Resistance by 2050? PLOS Med. 2016; 13:e1002184. [PubMed: 27898664]

[3]. Bragg, RR, Meyburgh, CM, Lee, J-Y, Coetzee, M. Potential Treatment Options in a Post-antibiotic EraInfect Dis Nanomedicine III Adv Exp Med Biol. Adhikari, R, Thapa, S, editors. Springer; Singapore: 2018. 51–61.

[4]. Chen Z, Ji H, Liu C, Bing W, Wang Z, Qu X. A Multinuclear Metal Complex Based DNase-Mimetic Artificial Enzyme: Matrix Cleavage for Combating Bacterial Biofilms. Angew Chemie Int Ed. 2016; 55:10732–10736.

[5]. Zhang Y, Sun P, Zhang L, Wang Z, Wang F, Dong K, Liu Z, Ren J, Qu X. Silver-Infused Porphyrinic Metal-Organic Framework: Surface-Adaptive, On-Demand Nanoplatform for Synergistic Bacteria Killing and Wound Disinfection. Adv Funct Mater. 2019; 29

[6]. Campoccia D, Montanaro L, Arciola CR. The significance of infection related to orthopedic devices and issues of antibiotic resistance. Biomaterials. 2006; 27:2331–2339. [PubMed: 16364434]

[7]. Lebeaux D, Ghigo J-M, Beloin C. Biofilm-Related Infections: Bridging the Gap between Clinical Management and Fundamental Aspects of Recalcitrance toward Antibiotics. Microbiol Mol Biol Rev. 2014; 78:510–543. [PubMed: 25184564]

[8]. Vallet-Regi M, Rámila A, del Real RP, Pérez-Pariente J. A New Property of MCM-41: Drug Delivery System. Chem Mater. 2001; 13:308–311.

[9]. Vallet-Regí M, Colilla M, Izquierdo-Barba I, Manzano M. Mesoporous Silica Nanoparticles for Drug Delivery: Current Insights. Molecules. 2017; 23:47.

[10]. Castillo RR, Lozano D, Gonzalez B, Manzano M, Izquierdo-Barba I, Vallet-Regi M. Advances in mesoporous silica nanoparticles for targeted stimuli-responsive drug delivery: an update. Expert Opin Drug Deliv. 2019; 16:415–439. [PubMed: 30897978]

[11]. Martínez-Carmona M, Gun'ko Y, Vallet-Regí M. Mesoporous Silica Materials as Drug Delivery: "The Nightmare" of Bacterial Infection. Pharmaceutics. 2018; 10:279.

[12]. González B, Colilla M, Díez J, Pedraza D, Guembe M, Izquierdo-Barba I, Vallet-Regí M. Mesoporous Silica Nanoparticles Decorated with Polycationic Dendrimers for Infection Treatment. Acta Biomater. 2018; 68:261–271. [PubMed: 29307796]

[13]. Pedraza D, Díez J, Isabel-Izquierdo-Barba, Colilla M, Vallet-Regí M. Amine-Functionalized Mesoporous Silica Nanoparticles: A New Nanoantibiotic for Bone Infection Treatment. Biomed Glas. 2018; 4:1–12.

[14]. Baptista PV, McCusker MP, Carvalho A, Ferreira DA, Mohan NM, Martins M, Fernandes AR. Nano-Strategies to Fight Multidrug Resistant Bacteria—"A Battle of the Titans,". Front Microbiol. 2018; 9

[15]. Niepa THR, Vaccari L, Leheny RL, Goulian M, Lee D, Stebe KJ. Films of Bacteria at Interfaces (FBI): Remodeling of Fluid Interfaces by Pseudomonas aeruginosa. Sci Rep. 2017; 7

[16]. Rüdiger, H. Isolation of Plant LectinsLectins Glycobiol. Gabius, H, Gabius, S, editors. Springer Berlin Heidelberg; Berlin, Heidelberg: 1993. 31–46.

[17]. Cummings, RD, Darvill, AG, Etzler, ME, Hahn, MG. Glycan-Recognizing Probes as Tools. 2015.

[18]. Dube DH, Bertozzi CR. Glycans in cancer and inflammation — potential for therapeutics and diagnostics. Nat Rev Drug Discov. 2005; 4:477–488. [PubMed: 15931257]

[19]. Martínez-Carmona M, Lozano D, Colilla M, Vallet-Regí M. Lectin-conjugated pH-responsive mesoporous silica nanoparticles for targeted bone cancer treatment. Acta Biomater. 2017; 65:393–404. [PubMed: 29127069]

[20]. Tang EN, Nair A, Baker DW, Hu W, Zhou J. In Vivo Imaging of Infection Using a Bacteria-Targeting Optical Nanoprobe. J Biomed Nanotechnol. 2014; 10:856–863. [PubMed: 24734538]

[21]. Jandú JJB, Moraes Neto RN, Zagmignan A, de Sousa EM, Brelaz-de-Castro MCA, dos Santos Correia MT, da Silva LCN. Targeting the Immune System with Plant Lectins to Combat Microbial Infections. Front Pharmacol. 2017; 8:1–11. [PubMed: 28149278]

[22]. Paunova-krasteva T, Stoitsova SR, Topouzova T. Escherichia coli O157 : Effects of growth temperature on concanavalin a binding and the adherence to cultured cells, Comptes Rendus l'Acad´emie Bulg. Des Sci. 2014; 64

[23]. Strathmann M, Wingender J, Flemming H. Application of fluorescently labelled lectins for the visualization and biochemical characterization of polysaccharides in biofilms of Pseudomonas aeruginosa. J Microbiol Methods. 2002; 50:237–248. [PubMed: 12031574]

[24]. Amine Ben Mlouka M, Cousseau T, Di Martino P. Application of fluorescently labelled lectins for the study of polysaccharides in biofilms with a focus on biofouling of nanofiltration membranes. AIMS Mol Sci. 2016; 3:338–356.

[25]. Vyas SP, Sihorkar V, Dubey PK. Preparation, characterization and *in vitro* antimicrobial activity of metronidazole bearing lectinized liposomes for intra-periodontal pocket delivery. Pharmazie. 2001; 56:554–60. [PubMed: 11487975]

[26]. Herigstad B, Hamilton M, Heersink J. How to optimize the drop plate method for enumerating bacteria. Journal of microbiological methods. 2001; 44:121–129. [PubMed: 11165341]

[27]. Grün M, Lauer I, Unger KK. The synthesis of micrometer- and submicrometer-size spheres of ordered mesoporous oxide MCM-41. Adv Mater. 1997; 9:254–257.

[28]. Cicuéndez M, Doadrio JC, Hernández A, Portolés MT, Izquierdo-Barba I, Vallet-Regí M. Multifunctional pH sensitive 3D scaffolds for treatment and prevention of bone infection. Acta Biomaterialia. 2018; 65:450–461. [PubMed: 29127064]

[29]. Wang Y, Baeyens W, Huang C, Fei G, He L, Ouyang J. Enhanced separation of seven quinolones by capillary electrophoresis with silica nanoparticles as additive. Talanta. 2009; 77:1667–1674. [PubMed: 19159781]

[30]. Forier K, Messiaen A-S, Raemdonck K, Nelis H, De Smedt S, Demeester J, Coenye T, Braeckmans K. Probing the size limit for nanomedicine penetration into Burkholderia multivorans and Pseudomonas aeruginosa biofilms. J Control Release. 2014; 195:21–28. [PubMed: 25125326]

[31]. Slomberg DL, Lu Y, Broadnax AD, Hunter RA, Carpenter AW, Schoenfisch MH. Role of Size and Shape on Biofilm Eradication for Nitric Oxide-Releasing Silica Nanoparticles. ACS Appl Mater Interfaces. 2013; 5:9322–9329. [PubMed: 24006838]

[32]. Rukavina Z, Vanić Ž. Current trends in development of liposomes for targeting bacterial biofilms. Pharmaceutics. 2016; 8

[33]. Noel GJ. A Review of Levofloxacin for the Treatment of Bacterial Infections. Clin Med Ther. 2009; 1

[34]. Klein RC, Fabres-Klein MH, Licursi De Oliveira L, Feio RN, Malouin F, De Oliveira Barros Ribon A. A C-type lectin from Bothrops jararacussu venom disrupts staphylococcal biofilms. PLoS One. 2015; 10:1–16.

[35]. Alyousef AA, Alqasim A, Aloahd MS. Isolation and characterization of lectin with antibacterial, antibiofilm and antiproliferative activities from Acinetobacter baumannii of environmental origin. J Appl Microbiol. 2018; 124:1139–1146. [PubMed: 29349932]

[36]. Vasconcelos MA, Arruda FVS, Carneiro VA, Silva HC, Nascimento KS, Sampaio AH, Cavada B, Teixeira EH, Henriques M, Pereira MO. Effect of Algae and Plant Lectins on Planktonic Growth and Biofilm Formation in Clinically Relevant Bacteria and Yeasts. Biomed Res Int. 2014; 2014:1–9.

[37]. Zaat SAJ, Broekhuizen CAN, Riool M. Host tissue as a niche for biomaterial associated infection. Fut Microbiol. 2010; 5:1149–1151.

[38]. Lu J, Liong M, Li Z, Zink JI, Tamanoi F. Biocompatibility, Biodistribution, and Drug-Delivery Efficiency of Mesoporous Silica Nanoparticles for Cancer Therapy in Animals. Small. 2010; 6:1794–1805. [PubMed: 20623530]

Europe PMC Funders Author Manuscripts

Europe PMC Funders Author Manuscripts

Statement of Significance

The present study is focused on finding an adequate therapeutic solution for the treatment of bone infection using nanocarriers that are capable of overcoming the biofilm barrier by increasing the therapeutic efficacy of the loaded antibiotic. For this purpose, we present a nanoantibiotic that increases the effectiveness of levofloxacin to destroy the biofilm formed by the model bacterium *E. coli.*. This work opens new lines of research in the treatment of chronic infections based on nanomedicines.

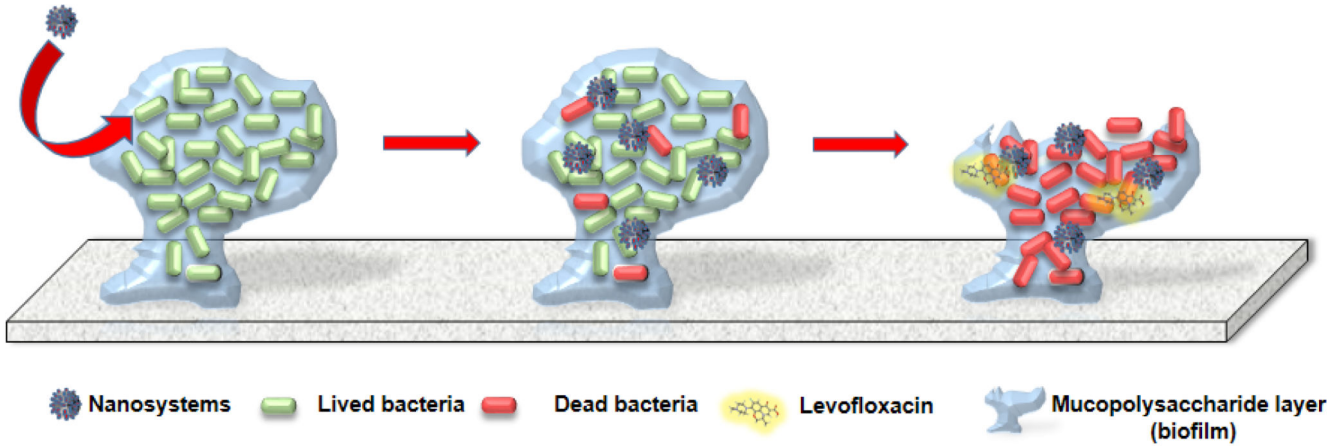

Fig. 1.
Schematic illustration of the aim of thisstudy.

Europe PMC Funders Author Manuscripts

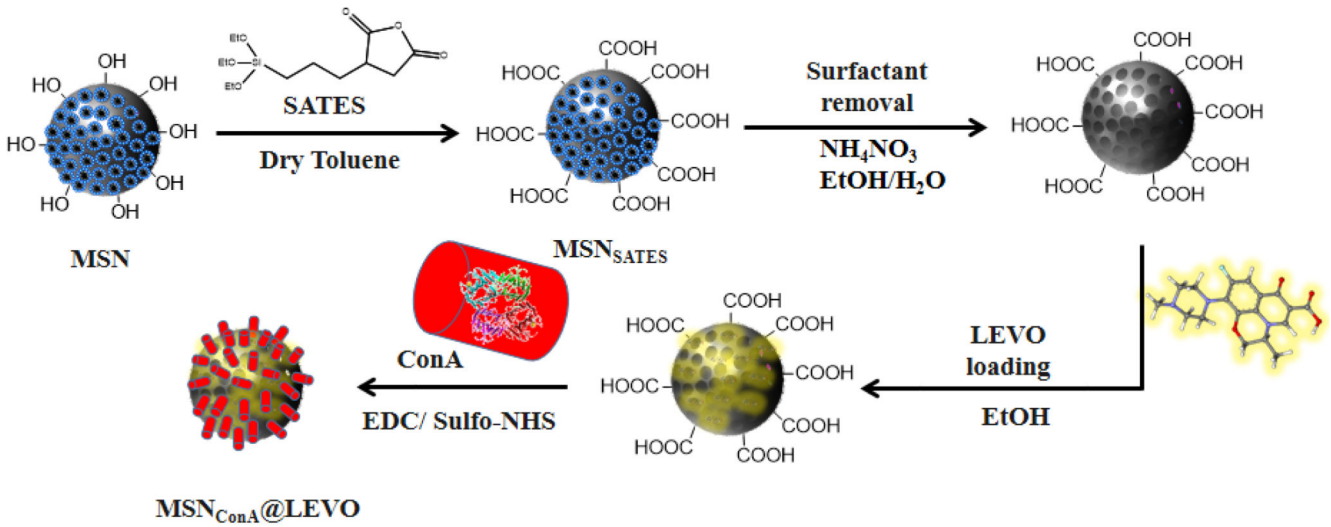

Fig. 2.

Schematic depiction of the synthesis procedure used to develop our nanoantibiotic: (i) Functionalization with carboxylic groups (MSN_{SATES}); (ii) surfactant extraction; (iii) loading of LEVO; (iv) anchoring of ConA into external surface of nanoparticles (MSN_{ConA}@LEVO).

Europe PMC Funders Author Manuscripts

Europe PMC Funders Author Manuscripts

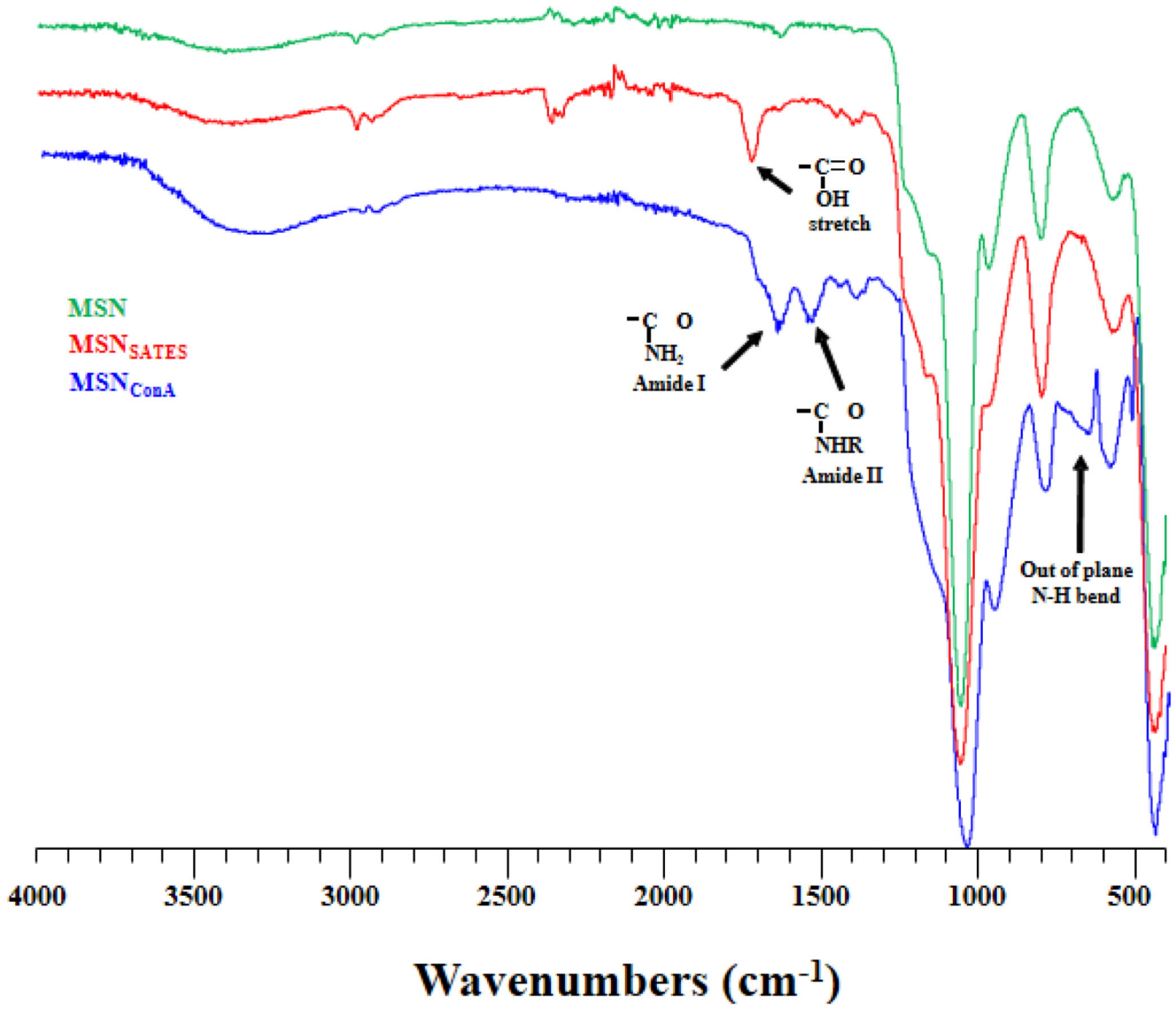

Fig. 3.

FTIR spectra of MSN, MSN$_{SATES}$, and MSN$_{ConA}$, confirming the effectiveness of the functionalization process.

Europe PMC Funders Author Manuscripts

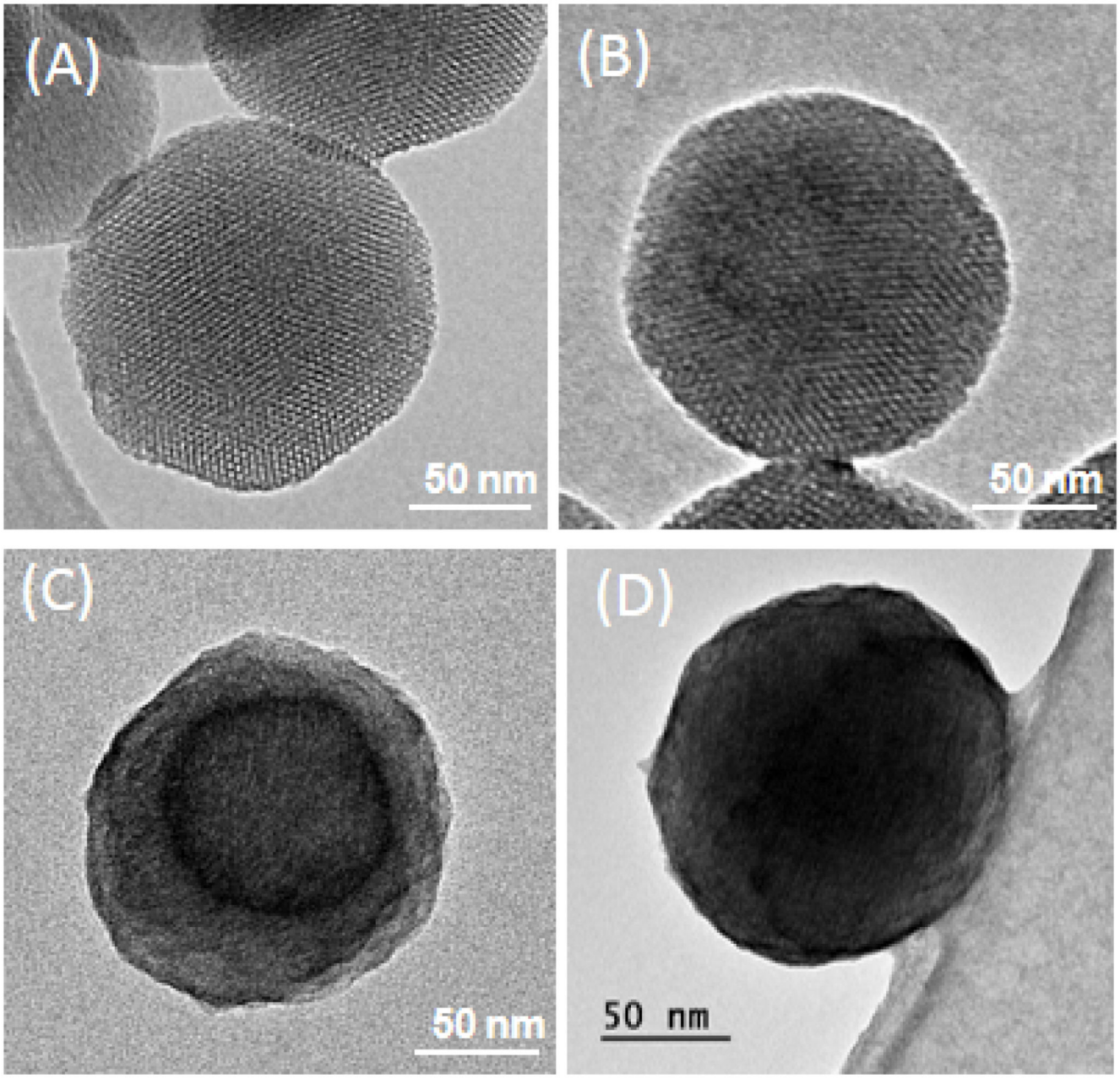

Fig. 4.

TEM images of (A) pristine MSN, (B) MSN_{SATES}, (C) MSN_{ConA}, and (D) MSN_{ConA}@LEVO, respectively. After functionalization with the organic compound, the samples were stained with 1% PTA for visualization by TEM (images C and D).

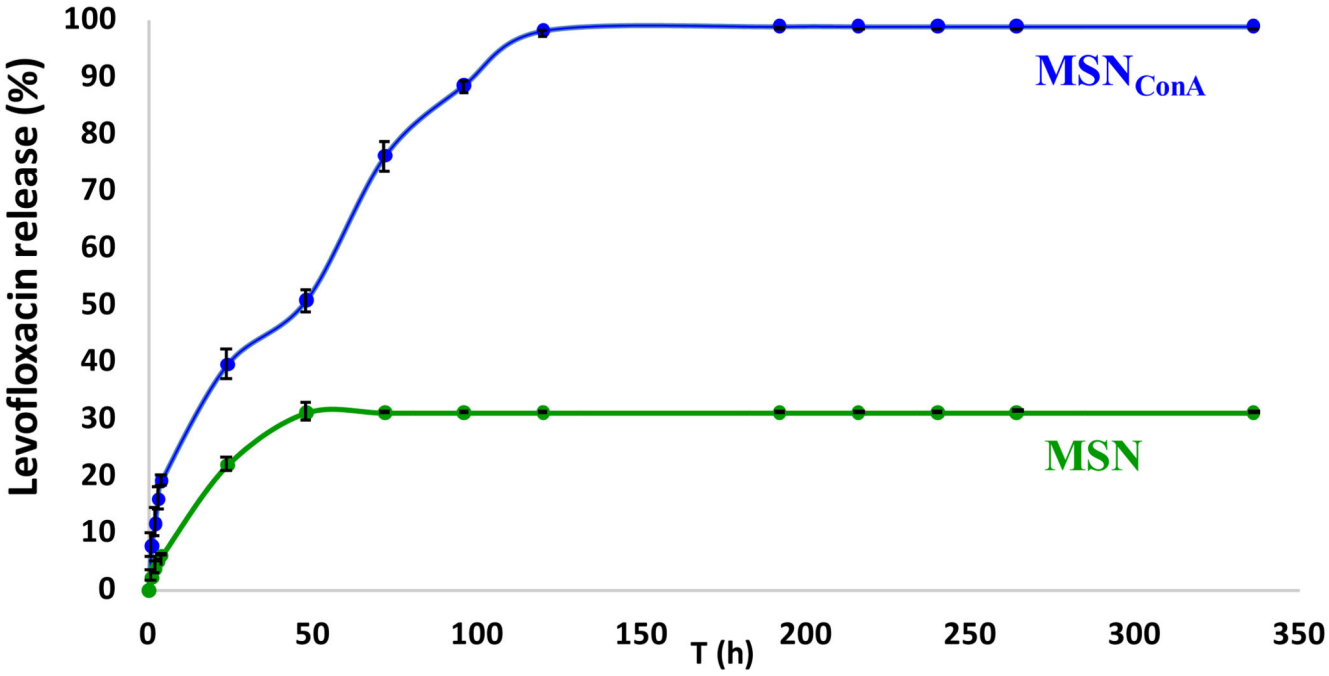

Fig. 5.

In vitro LEVO release profiles (n = 3) from MSN_{ConA} and MSN in PBS at 37ºC and orbital stirring. The amount of LEVO released was determined by fluorescence measurements of the solutions, (λex = 292 nm, λem = 494 nm) and expressed as accumulative drug release as function of time.

Europe PMC Funders Author Manuscripts

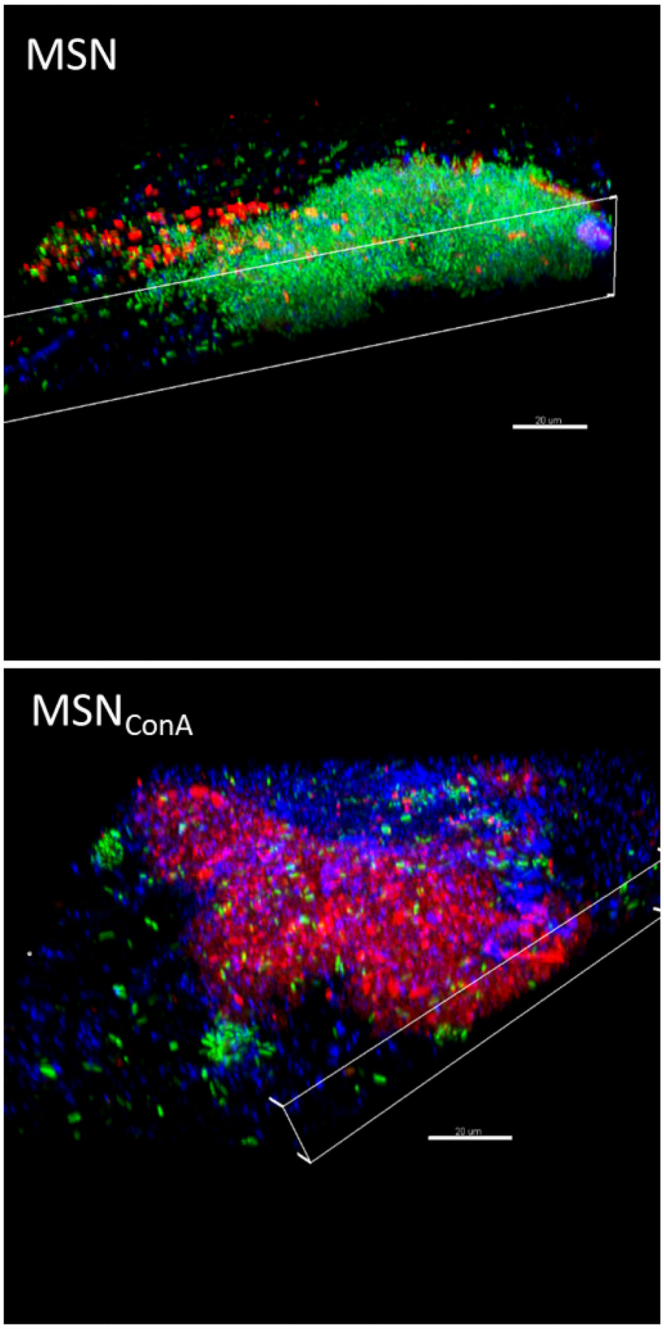

Fig. 6.

Confocal microscopy study of the internalization of red-labeled pristine MSN and MSN_{ConA} in preformed *E. coli* biofilms after 90 min of incubation with 50 μg/mL of nanoparticles. 3D confocal reconstruction shows that bare MSNs are localized onto the biofilm surface, whereas MSN_{ConA} penetrate the biofilm and are placed at different depth levels. Live bacteria are stained in green (SYTO), nanoparticles in red (RhB), and the extracellular polysaccharide biofilm matrix in blue (Calcofluor). Scale bars, 20 μm.

Europe PMC Funders Author Manuscripts

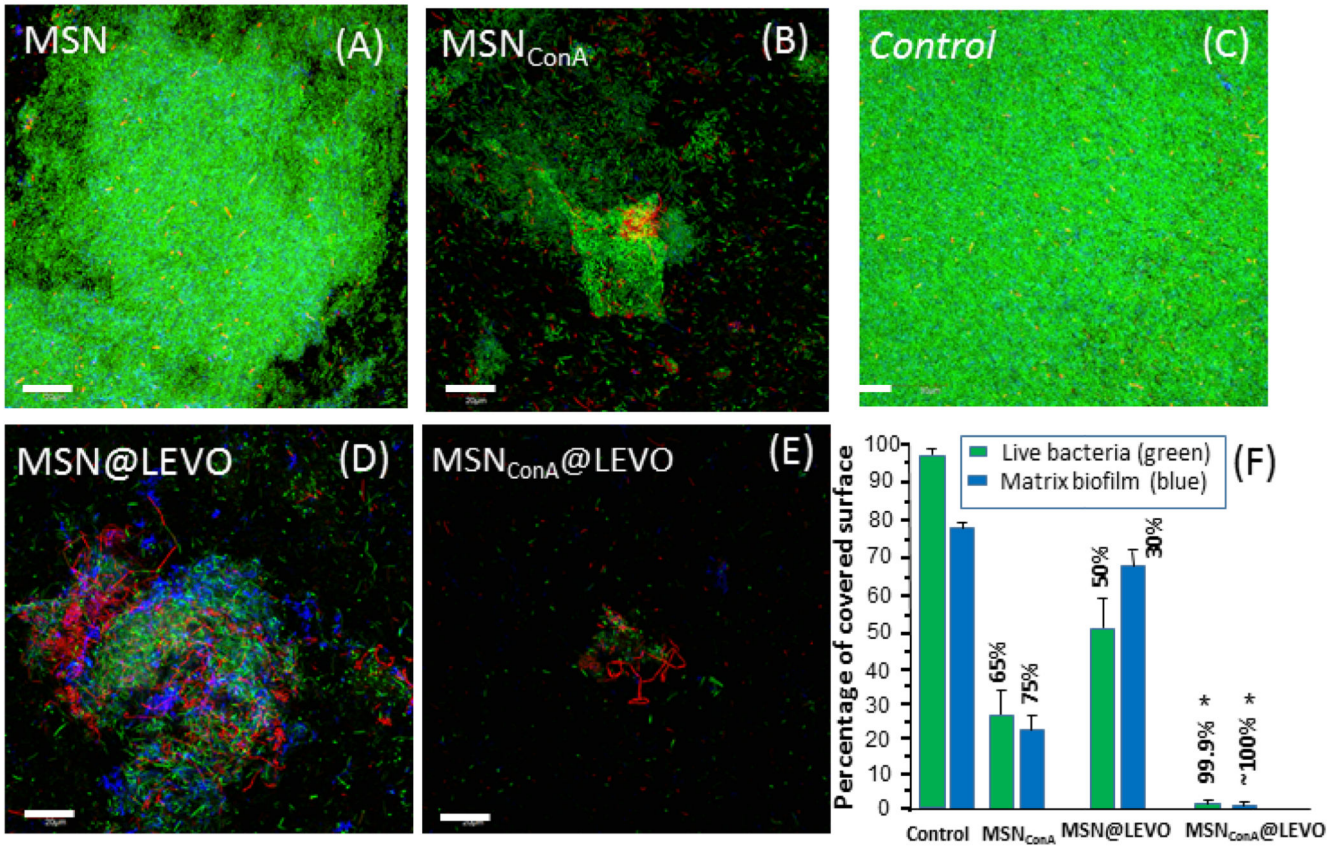

Fig. 7.

Confocal microscopy study of the antimicrobial activity of the LEVO-loaded MSN materials on the gram-negative *E. coli* biofilm. The images show (A) the biofilm preformed onto a covered glass disk without treatment (control) and after 90 min of incubation with (B) MSN@LEVO and (C) MSN_{ConA}@LEVO, respectively. Live bacteria are stained in green, dead bacteria in red, and the protective matrix biofilm in blue. Scale bars, 20 μm. (D) Histogram representing the percentage covered surface in green and blue from eight confocal images and calculated by ImageJ software (National Institutes of Health, Bethesda, MD) after treatment with 10 μg/mL of different nanoparticles. The numerical data represent the percentage of reduction in each case with regard to control (in the absence of any nanoparticle treatment). Experiments were performed in triplicate. *p <0.05 *vs.* corresponding MSN@LEVO and MSN_{ConA} (ANOVA).

Europe PMC Funders Author Manuscripts

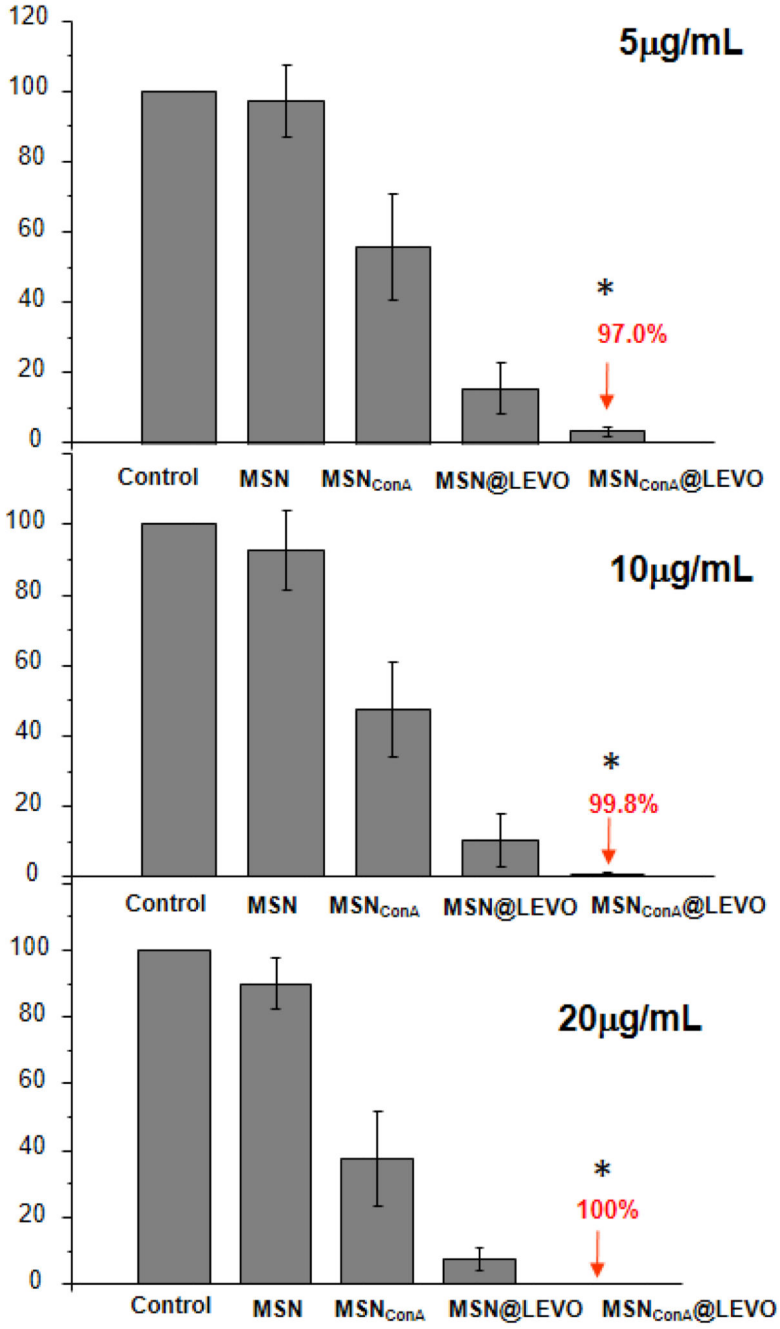

Fig. 8.

Effect of the samples on *E. coli* biofilm at different concentrations of the samples after 24 h. Results are represented as the reduction percentage with regard to control in the absence of nanoparticles. *p <0.05 *vs.* corresponding MSN@LEVO (ANOVA).

Europe PMC Funders Author Manuscripts

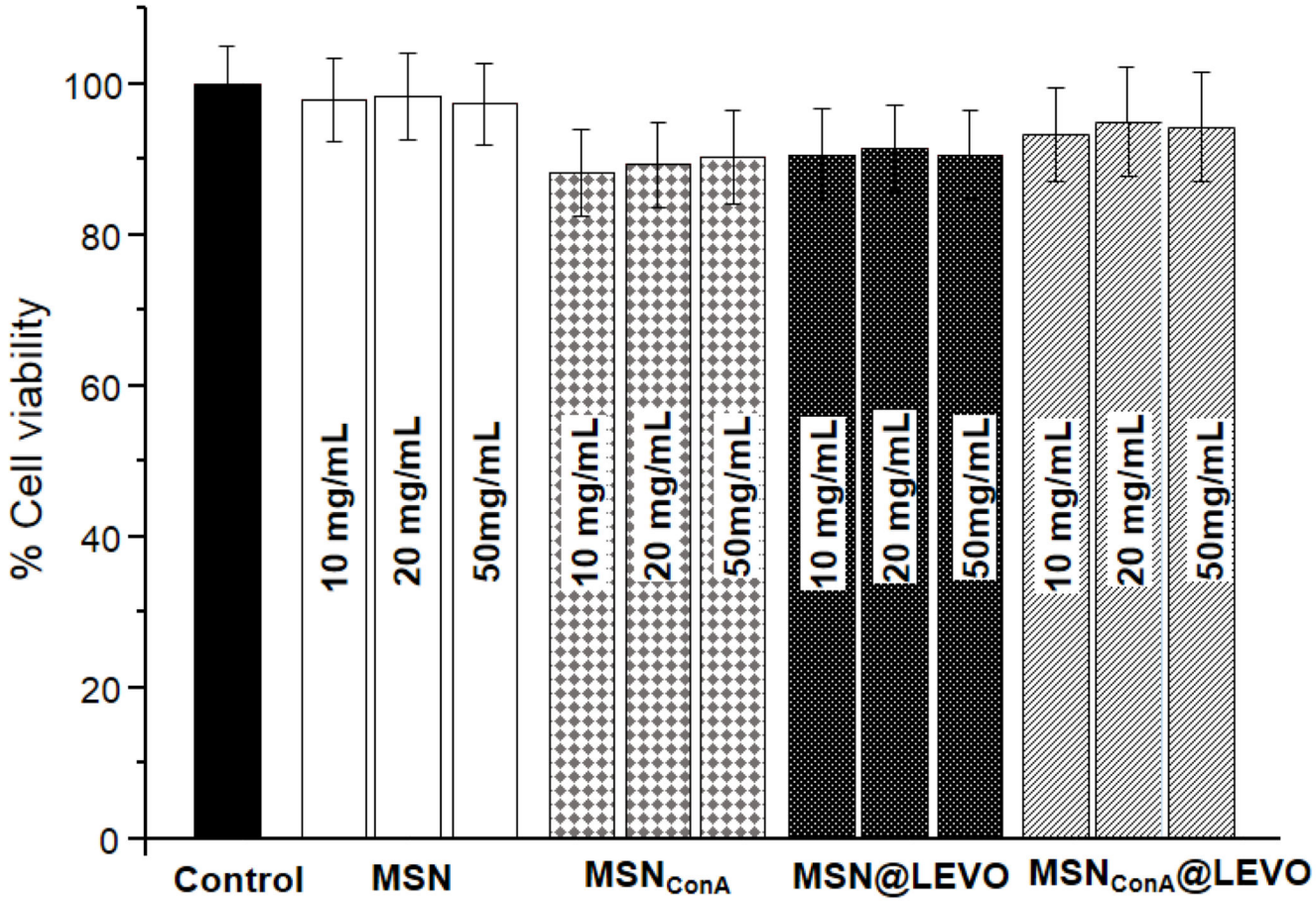

Fig. 9.

Cell viability studies of the samples at different concentrations for the MC3T3-E1 cell line with 24 h of exposure time. *p <0.05 *vs.* corresponding control without nanoparticles (ANOVA).